Epitaxial growth of $Si_{1-y}C_y$ alloys characterized as self-organized, ordered, nanometer-sized C-rich aggregates in monocrystalline Si

L. Simon
Laboratoire de Physique et de Spectroscopie Electronique, URA CNRS 1435, Faculté des Sciences, Université de Haute Alsace, 4 rue des Frères Lumière, 68093 Mulhouse Cedex, France
and Laboratoire de Physique et Applications de Semi-conducteurs, UPR-CNRS 292, 23 rue du Loess, 67037 Strasbourg Cedex 2, France

L. Kubler,* J. L. Bischoff, and D. Bolmont
Laboratoire de Physique et de Spectroscopie Electronique, URA CNRS 1435, Faculté des Sciences, Université de Haute Alsace, 4 rue des Frères Lumière, 68093 Mulhouse Cedex, France

J. Fauré
Laboratoire de Microscopie Electronique, Groupe de Recherche Surfaces et Matériaux, Université de Reims-Champagne-Ardennes, 21 rue Clément Ader, 51685 Reims Cedex 2, France

A. Claverie
Centre d'Elaboration des Materiaux et d'Etudes Structurales, CNRS, Boîte Postale 4347, 31055 Toulouse, France

J. L. Balladore
Laboratoire de Physique et Applications de Semi-conducteurs, UPR-CNRS 292, 23 rue du Loess, 67037 Strasbourg Cedex 2, France
(Received 13 March 1996)

Molecular-beam epitaxy deposition at 600 °C of Si in the presence of a C precursor (C_2H_4) allows us to identify, in specific kinetic conditions, a particular C accommodation mode in Si. By cross-sectional transmission electron microscopy we observe a precipitation of nanometric, highly supersaturated C-rich aggregates (1–3 nm) excluding silicon carbide or graphite formation. More surprisingly, these zero-dimensional aggregates are all self-organized in two-dimensional layers, parallel to the growth surface, and reveal a periodicity of about 9 nm, like in a ''natural'' superlattice. This indicates the occurrence of a cyclic, growth-induced carbon precipitation into a defect-free epitaxied Si matrix, forming a heterogeneous $Si_{1-y}C_y$ alloy, in spite of constant C and Si supplies all along the growth. The kinetic conditions governing this particular self-organization are specified in terms of Si and C impinging rates at the growth surface. Moreover, by x-ray photoelectron diffraction on the C 1*s* core level, we demonstrate that a local ordering, corresponding to that in the surrounding Si matrix, exists between the carbon atoms and their first Si neighbors inside the aggregates. This result provides major arguments in favor of the existence of the Si_nC phases recently predicted by *ab initio* calculations even if the observation of structured electron, forward-scattering events for next-nearest neighbors is hindered by probable distortions around the C atoms due to high local strain. Finally, the periodic C precipitation is explained on the basis of recently developed concepts of surface related C-solubility enhancements and sequential burying in C-enriched Si_nC phases of the accumulated C-rich surface layers. Such phases could prove more stable than diluted carbon when forced to match silicon. [S0163-1829(96)03336-X]

INTRODUCTION

Very recent reports[1–3] have raised intriguing questions about carbon incorporation into Si crystals. First, on the basis of theoretical calculations, Rücker *et al.*[1] predicted stoichiometric Si_nC phases ($n=3,4\ldots$, i.e., with C concentrations up to 25%) to be energetically more stable than C incorporation in isolated substitutional sites. Thus, in the case of the introduction of rather high C concentrations in $Si_{1-y}C_y$ alloys with y average values of a few percent, well above the bulk solubility limit of 10^{-4}% in a silicon matrix, these impurities would tend to condense into highly concentrated regions of ordered alloys with C concentrations locally as high as 25%.

More recently, Tersoff[2] payed particular attention to the theoretical discussion of the different driving forces that should lead to experimental growths of highly supersaturated solid solutions in general, the study being illustrated in particular by calculations of C in Si. The role of stress reduction in the strong increase of solubility and diffusion when C impurities are located near the surface is thus pointed out. This increase of surface solubility has been further supported recently by an x-ray photoemission spectroscopy examination by Osten *et al.*[3] on the C 1*s* core level of C atoms upon Si(001). Tersoff[2] also predicted, under specific kinetic conditions, the possible burying of such C-enriched surface regions during their growth, leading to a metastable material that would present very high levels of substitutional C throughout the bulk.

In this paper we provide experimental evidence for the aforementioned concepts in presenting, in a noninterrupted

growth process of $Si_{1-y}C_y$ alloys, a synthesis of metastable, ordered, C-rich phases, with concentrations in the range of that predicted by Rücker *et al.*,[1] embedded pseudomorphically in a grown defect-free Si monocrystal. As we have obtained this result in two different growth directions ([001] and [111]) and with two different C-gas precursors (CH_4 and C_2H_4) the relevant growth process seems to be rather general, provided delimited conditions for the growth kinetics are fulfilled. In this paper we restrict our description to the layers grown on Si(001) with C_2H_4. Our conclusions have been drawn from a number of experimental techniques, the most striking results being established by cross-sectional transmission electron microscopy (XTEM) and diffraction or x-ray photoelectron spectroscopy (XPS) and diffraction (XPD). Some preliminary results on this subject have been presented in Refs. 4 and 5.

These results present an obvious fundamental interest in offering insights into the accommodation mechanisms in Si matrices of a nonmiscible element as well as into the growth-governed formation of metastable phases. With a more practical view, this problem probably has important involvements in the field of elaboration of strained or strain-compensated $Si_{1-y}C_y$ and $Si_{1-x-y}Ge_xC_y$ alloys,[6,7] where only diluted substitutional C is desired and the formation of such phases is to be avoided, a fact that has not always been the case. The latter interest is motivated by the perspectives of band-gap tunability within Si-based heterostructures and the creation of tensile strain as opposed to the compressive strain occurring in the $Si_{1-x}Ge_x$ alloys.

EXPERIMENT

All $Si_{1-y}C_y$ layers are grown in an ultrahigh vacuum system, operating at base pressures in the 10^{-10}-mbar range, equipped with a Si electron-beam evaporator generating the Si molecular-beam epitaxy vapor flux and a C_2H_4 gas feed oriented onto a substrate whose temperature is varied by direct Joule heating and held at 600 °C during growth. External chemical treatments followed by repeated Ar^+ sputtering and 800 °C annealings are used to achieve a standard reconstructed Si(001) surface (ascertained by 2×1 low-energy electron diffraction spots) on which a Si buffer layer of about 60 nm is systematically deposited prior to the alloy $Si_{1-y}C_y$ layer growth.

Carbon supply is obtained by simple thermal dissociation of C_2H_4, the growth surface being held at 600 °C. The mean carbon incorporation (y) is varied for a given Si deposition rate, by selected C_2H_4 gas flows through a calibrated leak valve, controlled by the measure of the dynamical pressure in the growth chamber. Typically, Si deposition rates of 1.2 nm/mn or 0.2 Å/sec and C_2H_4 pressures between 10^{-6} and 6×10^{-6} mbar allowed the obtainment of y values of up to 8% as estimated within an absolute accuracy of 30% by computing the ratio of the XPS C 1s to Si 2p intensities. It should nevertheless be noticed that these concentrations are only representative of the surface termination of the films (inelastic mean free path of Si electrons $\lambda\sim20$–25 Å). That is why some of the mean C content over the whole thickness has also been checked with some secondary-ion-mass spectroscopy (SIMS) profiles. The carbon concentration is now found ranging from 0 to 2%, i.e., approximately reduced by a factor 4 in comparison to the XPS determinations. Reasons for this will be given later in the discussion of the growth mode. All XPS spectra are acquired using a Mg K_α radiation. As the polar angle θ of the analyzed electrons could be varied by rotation of the sample holder around a rotation axis coinciding with a ⟨100⟩ or ⟨110⟩ crystal axis, polar angle scans of the emitted-electron core-level intensities could be achieved. This technique, named XPD, provides surface crystallographic information. When XPD angular modulations can be observed, the local atomic environment can be derived.[8,9]

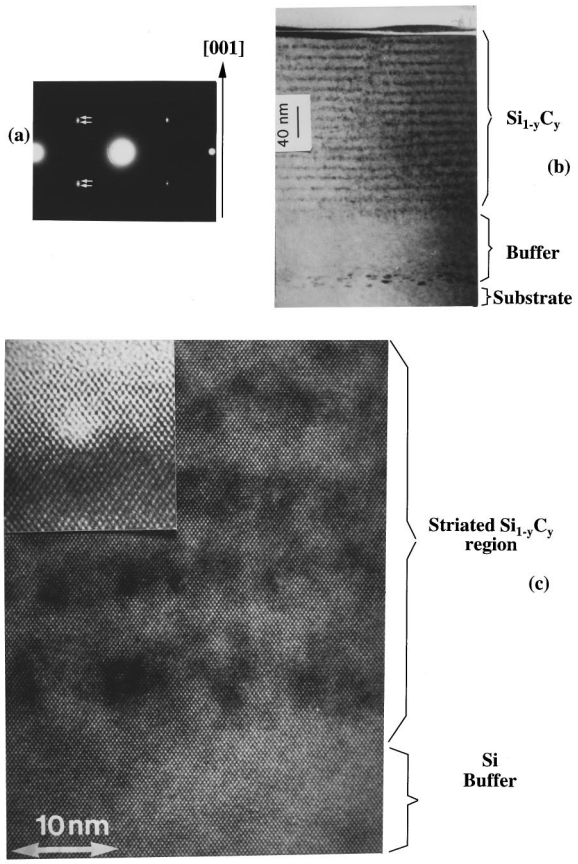

FIG. 1. (a) Electron-diffraction pattern of a typical $Si_{1-y}C_y$ layer grown at a C_2H_4 pressure of 3×10^{-6} mbar for which an XTEM bright field ⟨220⟩ image is given in (b) and showing periodic contrast variations parallel to the growth surface. (c) High-resolution view (HREM) zooming on several striated regions in proximity of the buffer layer. The inset is an enlarged image on a small precipitate of nanometric size. The arrows in (a) point towards two satellite spots, consequence of the C-rich pseudosuperlattice seen in (b) in the [001] growth direction.

Samples were prepared for XTEM examination using standard ion milling procedures. Classical and high XTEM investigations of the microstructure of the alloys were performed at 300 keV using a CM-30 Philips microscope.

RESULTS

Figure 1 strikingly illustrates the particular growth mode of our $Si_{1-y}C_y$ alloys provided defined kinetic growth conditions are used. In spite of a perfect monocrystalline growth with orientation relation with the Si(001) substrate, ascer-

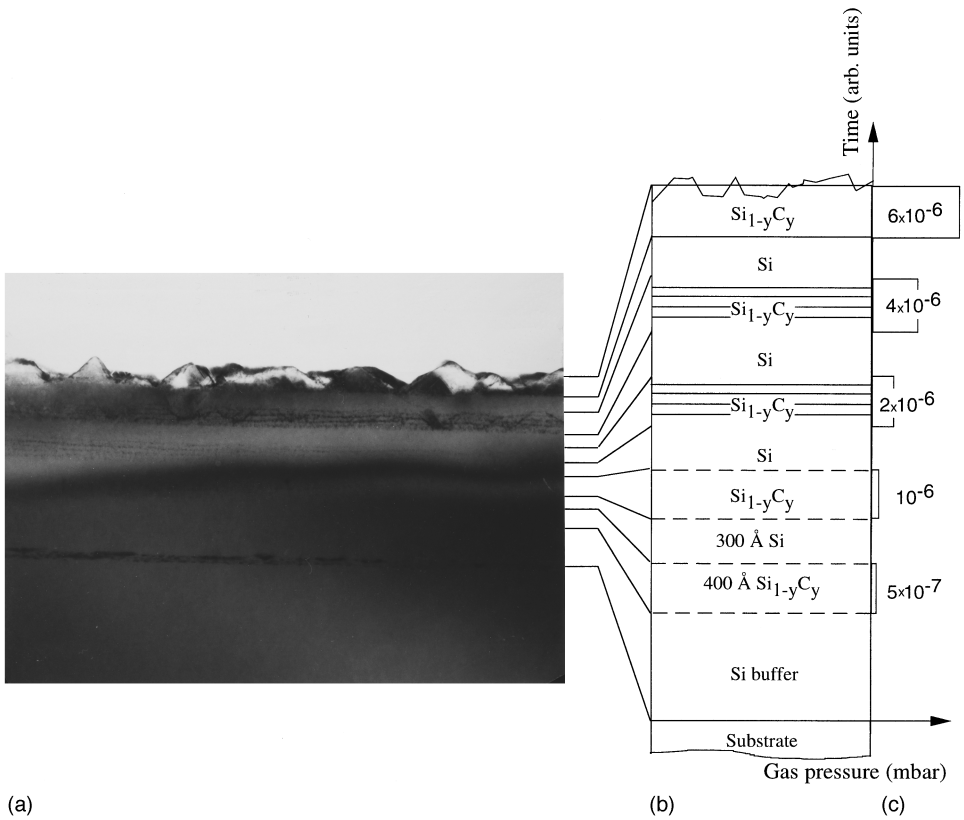

FIG. 2. (a) XTEM image in the (220) plane of five $Si_{1-y}C_y$ layers obtained by continuous layer growth at different C_2H_4 pressures spaced by Si buffer layers where C_2H_4 has been pumped down without any change in the Si evaporation flux. The detail of the growth procedure with the layer alternances is shown in (b), while (c) represents the time evolution of the gas pressure during the growth.

tained by the diffraction pattern given in Fig. 1(a), the deposited layer presents surprising contrast modulations or striations parallel to the surface [Fig. 1(b)]. Their apparent periodicity (9–10 nm with a standard deviation of 2 nm) is confirmed by the detection of satellite spots in the diffraction pattern in the [002] growth direction [Fig. 1(a)]. Further analyses by high-resolution electron microscopy (HREM) [Fig. 1(c)] evidence that the striations are made of a population of individual ''clouds'' of about 1–3 nm in diameter, which are distributed at discrete depths from the sample surface in the striated regions. Moreover, classical contrast analysis shows that these clouds have a mean atomic number that is smaller than the surrounding Si crystal, while neither evidence for strain around or within the clouds nor dislocations and SiC nanocrystal inclusions are to found after a weak-beam or HREM analysis. Thus these unexpected contrast variations, roughly periodic in the growth direction, may be interpreted as cyclic precipitation during the growth of aggregates of highly C-rich phases alternating with nearly pure and unstrained Si growth. The latter point is confirmed by an alloy-induced x-ray diffraction (XRD) [004] shift that is not in relation to the incorporated C amount. At this stage it should also be noticed that we obtain this oscillatory heteregeneous growth mode in a noninterrupted growth process characterized by *constant Si and C supplies*. Therefore, the generation of this oscillating behavior of the C accommodation must be the result of a growth-induced self-organization. Taking an averaged C composition for the layer of Fig. 1 of 1.5% and an approximative ratio $r \sim \frac{1}{15}$ between the cloud occupancy and the whole crystal volume, we derive a rough estimate for the C concentration in the enriched regions of $15 \times 1.5\% = 23\%$ for this given pressure of fabrication.

In Fig. 2 this particular growth mode is proven to be in close relation with the C arrival and to be possible only in a restricted domain of kinetic conditions. The TEM image in Fig. 2(a) corresponds to a multilayered preparation depicted schematically in Fig. 2(b) and consisting of sequential deposits of five different alloys obtained with increasing ethylene pressures (5×10^{-7}, 10^{-6}, 2×10^{-6}, 4×10^{-6}, and 6×10^{-6} mbar), the silicon deposition rate and the substrate temperature being kept constant throughout the whole deposit. Each individual alloy is 40 nm thick and, except for the last one, is spaced from the preceding and the following layer by 30-nm-thick Si buffer layers. Owing to this 40 nm individual thickness and to the periodicity between the C-rich regions seen in Fig. 1(b) (around 9 nm), about four striations could possibly be observable in the alloyed layers for which this striated growth mode would happen. In Fig. 2(a) it is possible to distinguish three layers presenting contrast oscillations corresponding to C_2H_4 pressures of 10^{-6}, 2×10^{-6}, and 4×10^{-6} mbar. As expected, we observe four striations in the two former layers. These striations are very weakly contrasted at 10^{-6} mbar and exhibit increasing contrasts at 2×10^{-6} and 4×10^{-6} mbar. Conversely, at the first probed pressure (5×10^{-7} mbar) the C incorporation rate must be too low to provoke striations as no C-rich region could be distinguished from the buffer layers. Otherwise, when the C_2H_4 pressure reaches 6×10^{-6} mbar, we obtain a breakdown of the monocrystalline growth, the upper layer becoming twinned [twins in the (111) planes]. Moreover, the growth is no longer bidimensional as three-dimensional (3D) islands are clearly seen in the top layer, some of them still presenting strongly contrasted striations. This trend towards creation of extended defects already appears at 4×10^{-6} mbar, where some twins can be observed. Below this pressure value, both buffer and alloyed layers are monocrystalline and quasi-defect-free.

Thus the major information from these experiments is that the particular defect-free formation of easily observable C-rich phases is severely shrunk in a restricted C_2H_4 pressure range (from 2 to 4×10^{-6} mbar), i.e., in a determined range of C arrival with respect to the Si impinging at the surface. In this domain, C-rich regions appear as periodic striations with a periodicity of about 9 nm, only weakly pressure dependent, with a best observation near 3×10^{-6} mbar, as previously experimented[4] (Fig. 1). Such a pressure corresponds to an approximate impinging rate of 1.7×10^{15} C atoms/cm^2 sec to be compared to 1×10^{14} Si atoms/cm^2 sec at a deposition rate of 0.2 Å/sec. As the flux of the carbon effectively incorporated for $y=1.5\%$ is about 1.7×10^{12} cm^{-2} sec^{-1}, the efficiency of C incorporation using C_2H_4 is about 10^{-3} per collision. This weak value is in good agreement with that of Cheng, Choyke, and Yates,[10] who explain it by C_2H_4 dissociation inefficiency and partial desorption on the Si surface states. We can also observe that our values of impinging C and Si fluxes are quite comparable with those utilized by Faschinger *et al.*[11] for electron-gun-generated C and Si sequential deposits. They allowed the characterization by high-resolution XRD of ''man-made'' alternating defect-free silicon and C-rich phases very similar to our ''natural'' alternaces directly visualized by TEM. It must also be noticed that the overall deposition rate allowing the obtention of our original growth mode (0.2 Å/sec) is significantly lower than those used in the more conventional chemical vapor deposition methods leading to substitutional C accommodation.

The general relationship of the striated regions with the impinging rate of the C precursor being now well established, we have to determine in the following whether the C-rich regions are ordered and how these striations grow. A set of further techniques provided complementary information about these samples, especially about the local order. The after-growth XPS analyses[4] reveal a C 1*s* core level, ascertaining the C incorporation, whose binding energy (283.2 eV) is near that of C atoms four-fold bonded with Si first neighbors as in SiC and rules out the presence of C-C or C-H bonds. In addition, the presence of only a slight Si 2*p* linewidth increase without any resolved component is inconsistent with SiC precipitation.[9] This point is further corroborated by ir and Raman analyses[4] showing no SiC components near 800 cm^{-1}. Only a weak component in the vibration region of the expected C local mode (604 cm^{-1}) has been observed.[4] It is slightly shifted towards higher frequencies with respect to this ideal substitutional value and may agree with the recently determined vibration contributions[12] in the C-rich Si_nC phases predicted by Rücker *et al.*[1] Such an argument in favor of ordered phases is nevertheless rather uncertain owing to the weakness of this signal. That is why we performed angular profiles on C 1*s* and Si 2*p* core-level intensities (or XPD) allowing the local probing of the relevant C and Si atoms, as forward focusing, which is a dominant result of the interference process between an emitted electron wave with scattered waves by the neighboring atoms, enhances electron emission in the direction of the atomic rows when monocrystals are analyzed. The obtainment of structured Si 2*p* patterns on the alloy surface, similar to the substrate distribution, provided further proof of the epitaxial growth outside the C-rich regions, which was described in a previous paper.[4] We want to focus now on the possibility of obtaining XPD modulations on C atoms that would also ascertain the ordered character inside the C-rich aggregates seen by HREM. Such measurements on an element with a low photoionization cross section and with a mean abundance in the alloy of 1–2 % are rather difficult to perform. These facts, together with growth-related reasons that will be explained below, had hampered the observation of clearly structured C 1*s* profiles in our previous paper[4] on the surface termination of a thick $Si_{1-y}C_y$ alloy.

As the C-rich phase formation is proved to be periodic (9-nm period), we can now accurately follow with our *in situ* photoemission techniques the growth mechanism leading to the emergence of the first striation. For this purpose, we performed C 1*s* and Si 2*p* XPD patterns for $Si_{1-y}C_y$ films of increased thicknesses, by steps of 20 Å, in the thickness range of interest for the first striation appearance, i.e., from 0 to 100 Å. We thus expect to select, in the XPS probing depth, at a given thickness the first appearance of the precipitation phenomenon and the start of the possible ordering in aggregates, which should be more difficult to observe at the termination of a thick layer owing to the irregularities in the striations [Fig. 1(b)] combined with lateral integration of the photoemission signal.

In Fig. 3(a) we first give a reminder of the XPD polar angle pattern of the Si(001) substrate probing the atomic arrangement in a (110) plane, the angular modulations at $\theta=0°$ and 55° corresponding to enhanced electron scattering in the [001] and [111] directions, respectively.[4,9] The distribution in Fig. 3(b) accounts for the same Si 2*p* peaks from Si atoms in a thick alloyed layer. The similarity of the pattern to the substrate indicates the same structural ordering. In the inset of Fig. 3 the quantified contrast f of [111] forward-scattering Si 2*p* feature is also presented as a function of the same alloy thickness. This curve is a measure of the evolution of the structural quality within the first ten monolayers in the growth front region at different growth stages leading to a striated layer.

The following distributions [Figs. 3(c)–3(g)] are relative to the C 1*s* peak in $Si_{1-y}C_y$ layers with increasing nominal thicknesses. They probe the local order evolution around C atoms during the first stages of the growth process. Up to a thickness of 60 Å, these distributions are featureless, indicating no ordering. This observation can be linked to the decrease in the same thickness range of the Si 2*p* contrasts (inset of Fig. 3), proving a crystalline quality degradation of the first-stage alloy deposit. Moreover, owing to the nearly unmodified instrumental function that is rapidly increasing with polar angle θ, the carbon atoms must constantly be located in the surface layers. This rapid increase is due to the surface sampling effect, varying as $1/\cos\theta$ does, with an increasing electron emission angle θ relative to the sample normal. The overall C 1*s* signal intensity increases with thickness, the angular shape remaining approximately unchanged. This demonstrates that more and more C, bonded with silicon, is accumulated in subsurface sites in the first layers as the growth proceeds from 0 to 60 Å. Indeed, accumulation of all carbon atoms exclusively in the top layer would probably lead to higher binding C 1*s* energies than those observed, which are more characteristic of bulk environments. This first stage is fully in accordance with

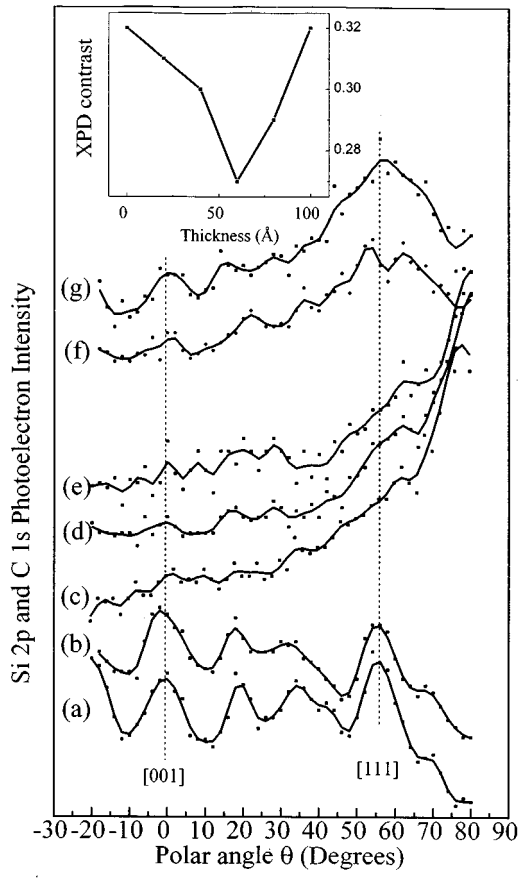

FIG. 3. XPS core-level angular distributions scanned in the (110) plane for (a) Si $2p$ electron emission from the Si substrate, (b) Si $2p$ electron emission from a 100-Å $Si_{1-y}C_y$ alloyed overlayer, and (c)–(g) C $1s$ electron emission from different alloy thicknesses: (c) 20 Å, (d) 40 Å, (e) 60 Å, (f) 80 Å, and (g) 100 Å. The solid lines are deduced from the experimental points using a smoothing program. In the inset the contrast or anisotropy factor f for the Si $2p$ polar distribution is represented as a function of the alloy thickness. The factor f is defined as $\Delta I/I_{\max}$, where ΔI is the intensity variation between the peak at $\theta=55°$ and the first minimum.

Tersoff's[2] point of view in favor of large C solubility extending over several near-surface layers (fewer than six monolayers) and confirms the main finding of Osten *et al.*[3]

Nevertheless, the point is that, for thicknesses above 60 Å, the Si $2p$ contrast starts to increase again (inset of Fig. 3), recovering its perfect substrate value, in connection with the emergence, for 80 and 100 Å [distributions (f) and (g) in Fig. 3], of a broad forward focusing feature in the C $1s$ polar distribution near 55°, i.e., in the angular region of the [111] direction of the diamond structure and the C first neighbors. This emergence is associated with a slower increase of the instrumental function, reflecting now the enhanced in-depth distribution of the C atoms. These observations indubitably prove the occurrence of a reordering stage of the C and Si atoms following an initial stage where only C is accumulated in near-surface Si layers. The nearest neighbors of the C atoms are now all mainly aligned in bonding directions matching the Si crystal. Thus, at a critical point of the growth, the C-enriched overlayers are subjected to a self-organized reordering in the buried clouds seen by XTEM. This reordering allows subsequent regrowth of nearly perfect, unstrained Si layers presenting higher XPD contrasts followed by a new stage of C accumulation up to the next precipitation into the C-rich phases. The periodic behavior of the C incorporation may thus find an explanation. In addition, as first-neighbor alignments around the C atoms are observed, these C-rich phases may correspond to Si_nC phases predicted by Rücker *et al.*,[1] of which only one characterization attempt, as far as we know, has been done to date.[13] Unfortunately, up to now we have failed to observe forward-focusing events corresponding to more distant ordered scatterers. The limited size of the atomic chains in our small aggregates, together with probable second- and third-neighbor desalignments due to strong local distortions induced by the C strain, may explain this absence.

At this stage of understanding of the original growth mode characterized here as an oscillatory C incorporation scheme alternating with periodic C surface enrichments, it must be noted that C concentration as deduced by XPS C $1s$ core-level intensity measurements is only rarely representative of the mean C content and must be overestimated. Thus the XPS deduced y values are probably not indicative of the true mean content and the discrepancy with SIMS values may be explained.

Otherwise, in spite of unquestionable interplays of our growth scheme with the concepts developed by Tersoff and Osten *et al.*, marked differences are also noticeable. Our most original finding consists of sequential freezing into the bulk of the supersaturated surface regions, a fact not predicted by Tersoff,[2] who suggested continuous burying. Additionally, our precipitates are organized in the 2D layers in a 0D form, at variance with the continuous 2D layers seen by Ruvimov *et al.*[12] Thus the thought that periodic precipitation is governed only by the attainment of the C surface solid solubility limit is probably inadequate. Indeed, in spite of higher C incorporations obtained by increasing C_2H_4 growth pressures, the striation period seems only weakly pressure dependent. Conversely, the contrasts of each striation set appear to be more marked, which reflects an increase of the C content in each 2D region of C-rich precipitation. The latter increase may be due to a higher aggregate density in the 2D region or a higher C concentration in each aggregate, their density remaining constant. This question that should be cleared up by intended high-resolution examinations may help know all driving forces leading to the precipitation for which the elastic strain energy necessary to stabilize these pseudomorphic C-rich phases must play a role. We plan to report on the occurrence of similar growth processes on the Si(111) face. Moreover, recent observations made by other authors prove that such natural oscillatory growth schemes seem to be a rather general phenomenon not limited to the silicon-carbon system. Thus Norman *et al.*[14] have reported on their ability to grow natural, i.e., growth-induced, $InAs_{0.5}Sb_{0.5}$ superlattices.

Recently Tillack *et al.*[15] and Radamson *et al.*[16] observed similar organizations with boron, another light element, in Si, while Herbots *et al.*[17] encountered inhomogeneous C distributions in $Si_{1-x-y}Ge_xC_y$ ternary alloys. The latter authors explain the formation of their C-rich phases by a ripening process on the basis of a stronger coarsening of the clusters

nearer to the substrate interface. Such a growth time dependence of the C-rich cluster size is by no means observed in our case, which presents [Fig. 1(b)] regularly sized precipitates throughout the layer, excluding such ripening process. Further investigations are needed in order to reach a better crystallographic characterization of the nanometric aggregates as well as to understand the exact physical mechanisms driving the periodic formation of the C-rich phases.

*Author to whom correspondence should be addressed. Fax: (33)89596359. Electronic address: L.KUBLER@univ-mulhouse.fr

[1] H. Rücker, M. Methfessel, E. Bugiel, and H. J. Osten, Phys. Rev. Lett. **72**, 3578 (1994).

[2] J. Tersoff, Phys. Rev. Lett. **74**, 5080 (1995).

[3] H. J. Osten, M. Methfessel, G. Lippert, and H. Rücker, Phys. Rev. B **52**, 12 179 (1995).

[4] M. Diani, L. Kubler, J. L. Bischoff, J. J. Grob, B. Prévot, and A. Mesli, J. Cryst. Growth **157**, 431 (1995).

[5] A. Claverie, J. Fauré, J. L. Balladore, L. Simon, A. Mesli, M. Diani, L. Kubler, and D. Aubel, J. Cryst. Growth **157**, 420 (1995).

[6] S. S. Iyer, K. Eberl, M. S. Goorsky, F. K. LeGoues, J. C. Tsang, and F. Cardone, Appl. Phys. Lett. **60**, 356 (1992); S. S. Iyer, K. Eberl, M. S. Goorsky, J. C. Tsang, F. K. LeGoues, F. Cardone, and B. A. Ek, in *Amorphous and Crystalline Silicon Carbide IV*, edited by C. Y. Yang, M. M. Rahman, and G. L. Harris, Springer Proceedings in Physics Vol. 71 (Springer, Berlin, 1992), p. 13.

[7] P. Boucaud, C. Francis, A. Larré, F. H. Julien, J. M. Lourtioz, D. Bouchier, S. Bodnar, and J. L. Regolini, Appl. Phys. Lett. **66**, 70 (1995).

[8] C. S. Fadley, Prog. Surf. Sci. **16**, 275 (1984).

[9] M. Diani, J. L. Bischoff, L. Kubler, and S. Bolmont, Appl. Surf. Sci. **68**, 575 (1993).

[10] C. C. Cheng, W. J. Choyke, and J. T. Yates, Surf. Sci. **231**, 289 (1990).

[11] W. Faschinger, S. Zerlauth, J. Stangl, and G. Bauer, Appl. Phys. Lett. **67**, 2630 (1995).

[12] H. Rücker, N. Methfessel, B. Dietrich, K. Pressel, and H. J. Osten, Phys. Rev. B **53**, 1302 (1996).

[13] S. Ruvimov, E. Bugiel, and H. J. Osten, J. Appl. Phys. **78**, 2323 (1995).

[14] A. G. Norman, T. Y. Seong, I. T. Ferguson, G. R. Booker, and B. A. Joyce, Semicond. Sci. Technol. **8**, S9 (1993).

[15] P. Tillack, P. Zaumseil, G. Morgenstern, D. Krüger, and G. Ritter, Appl. Phys. Lett. **67**, 1148 (1995).

[16] H. H. Radamson, K. B. Joelsson, W. X. Ni, L. Hultman, and G. V. Hansson, J. Cryst. Growth **157**, 80 (1995).

[17] N. Herbots, P. Ye, H. Jacobsson, J. Xiang, S. Hearne, and N. Gave, Appl. Phys. Lett. **68**, 782 (1996).